Assessing uncertainties in climate change impacts on resource potential for Europe based on projections from RCMs and GCMs

Stefan Fronzek[*] and Timothy R. Carter

Finnish Environment Institute, Box 140, FIN-00251 Helsinki, Finland

* Corresponding author: stefan.fronzek@ymparisto.fi, tel +358 20 490 2301, fax +358 9 4030 0390

Abstract

An analysis is presented of the estimated impacts of climate change on resource potential in Europe under a wide range of model-based climate scenarios. Simple models and indices were used to assess impacts on the growing season, potential biomass, thermal suitability for the cultivation of crops, and potential energy demand for indoor cooling. Impacts were estimated for climate during the 1961-1990 baseline period (both observed and modelled) and projected during 2071-2100 based on outputs from a range of regional climate models (RCMs) driven by general circulation models (GCMs) assuming forcing by SRES emission scenarios A2 and B2, and from six atmosphere-ocean GCMs forced by a wider range of emission scenarios.

Uncertainties in the projected impacts of climate change are assessed with respect to: 1) the direct climate model output vs. delta change approach, 2) differences in the driving GCMs and the RCM runs, 3) differences across a range of emission scenarios, 4) changes in long-term mean climate, and 5) changes in inter-annual climate variability.

Future simulations show substantial changes in all analysed impact sectors, but with a relatively large spread of results attributable to uncertainties in future climate expressed by the different scenarios. Results included shifts of the northern limits of areas thermally suitable for the cultivation of soya bean and grain maize by several hundred kilometres, lengthening of the thermal growing season by three to twelve weeks, strong increases of potential biomass in northern Europe and slight decreases in southern Europe, and increased energy demand for cooling throughout Europe.

Our results hint at systematic differences between RCM and GCM projections of temperature, though not precipitation, over Europe. The results also highlight the importance of accounting for inter-annual variability in estimating future impacts, through its affect on levels of risk. However, the results caution against the use of direct RCM outputs in impact models, due to biases in the representation of present-day climate. The delta change approach still appears to be the preferred option for most applications.

1. Introduction

Climate influences and determines processes in natural and human systems in various ways. This has been demonstrated by the wide range of impacts observed in recent decades related to regional warming in many parts of the world (IPCC, 2001). Recent examples of observed impacts from Europe include advances in the timing of spring events such as the leafing of trees (Chmielewski and Rotzer, 2001), lengthening of the growing season (Menzel et al., 2003) and latitudinal/altitudinal shifts in the distribution of species (Walther et al., 2002).

There have been numerous studies to estimate the potential impacts of future climate change across a large number of sectors in Europe (Parry, 2000; Kundzewicz et al., 2001). These impact studies are commonly based on climate projections by atmosphere-ocean general circulation models (AOGCMs). However, the great majority of studies apply scenarios from only a limited number of GCMs (exceptions include Hulme et al., 1999; Parry, 2000). This is despite acknowledged uncertainties in climate projections, attributable to model parameterisations, model structure, systemic internal variability, and forcing assumptions (McAvaney et al., 2001).

The horizontal spatial resolution of AOGCMs, with grid spacing in the order of about 300 km, is still much coarser than the driving processes of many impacts (Giorgi et al., 2001). This has led to repeated calls for higher resolution information to serve the impacts community (e.g. Mearns et al., 2001). One method to narrow the gap in spatial resolution is through dynamical downscaling of the GCM output, using regional climate models (RCMs) and other high resolution modelling techniques. The PRUDENCE project is the first to conduct a co-ordinated set of high resolution experiments for Europe at horizontal grid resolutions of about 50 km (Jacob et al., this volume). However, high resolution modelling introduces its own set of uncertainties (Giorgi et al., 2001), and the PRUDENCE project provides one of the first opportunities to test the utility of such models in a range of impact applications. This paper reports the results from an impact study with the following four objectives:

1. to apply the full set of PRUDENCE high resolution projections to simple indices of resource potential, relating to agriculture (growing season and crop suitability), ecosystems (potential biomass), and energy demand (cooling degree-days);

2. to analyse impacts estimated using different methods of climate scenario construction and application for baseline (1961-1990) and future (2071-2100) climates;

3. to evaluate the relative sensitivity of impacts to future changes in mean climate *vs*. changes in inter-annual variability; and

4. to compare impacts estimated using high resolution models with those estimated using a range of GCMs, under different assumptions of future emissions, in order to weigh the merits of applying alternative model-based scenarios to determine impacts.

2. Material and methods

2.1 Climate scenario construction

The baseline climate for the Europe-wide analysis of resource potential comprised interpolated monthly observations for 1961-1990 on a 0.5° latitude x 0.5° longitude grid from the Climatic Research Unit (CRU), University of East Anglia, (New et al., 1999, 2000, updated). Mean monthly temperature and precipitation were required for the analyses. Three types of climate projection were applied in the study (Table 1), each interpolated to the CRU grid for Europe at a monthly resolution for the 1961-1990 and 2071-2100 periods:

1. Outputs from 16 RCM simulations nested in two different GCM simulations, from six stretched-grid simulations [1], and from one of the driving GCM simulations (HadAM3H), all carried out in the PRUDENCE project (Jacob et al., this volume)

2. Outputs from six coupled AOGCMs for the SRES A2 and B2 emissions scenarios, obtained from the Intergovernmental Panel on Climate Change Data Distribution Centre (IPCC DDC[2]).

3. Outputs for the six AOGCMs described above, which had been pattern-scaled to represent regional climate under the SRES A1FI (highest) and B1 (lowest) emissions scenarios (Ruosteenoja et al., this volume).

Projections of summer (June-August) mean changes in temperature and annual changes in precipitation from a sample of models are summarised for northern and southern Europe as scatter plots in Figure 1.

---

[1] A GCM experiment run at a variable horizontal resolution across the globe ("stretched grid"), with the highest resolution over the region of interest, in this case Europe.

[2] http://ipcc-ddc.cru.uea.ac.uk

In all the applications reported here, the absolute difference between modelled present-day (1961-1990) and future (2071-2100) climate was added to the CRU observed baseline for both temperature and (where applicable) precipitation (delta change approach). Where inter-annual temperature variability was also required, model-based scenarios for individual years were calculated by applying the temperature anomaly (modelled individual year minus modelled baseline period-mean) to the CRU observed baseline period-mean temperature, equivalent to applying the delta change approach to period-mean climate and then adding modelled variability.

2.2 Impact models

The impact models chosen for this study are well established indices that describe climatic constraints on different ecosystem processes and human activities (resource potential). Three are based on air temperature (crop suitability, growing season and cooling degree-days) and one uses both temperature and precipitation (Miami Model). The models were intentionally selected to be simple, both to facilitate the rapid analysis of multiple scenarios (cf. Table 1) and to allow relative transparency in the interpretation of the results. More complex impact models have also been applied in PRUDENCE and are presented elsewhere (e.g. Olesen et al., this volume).

2.2.1 Thermal suitability for crops

Crops require sufficient warmth to develop through their phenological stages. The effective temperature sum (ETS), sometimes referred to as growing degree-days after its measurement units (°Cd), has been used to quantify this requirement. It is defined as the seasonal accumulation of mean daily temperatures above a given base temperature. It is applied here to calculate the thermal suitability for crop development and elsewhere in this paper as a proxy for the potential

6

energy demand for cooling (see section 2.1.3). While ETS is defined on the basis of daily temperatures, the temperature data required for this study were available only at a monthly resolution. We used a method suggested by Kauppi and Posch (1988) to estimate ETS using monthly mean temperatures, in which the ETS function is integrated over an assumed Gaussian daily temperature distribution. The method requires standard deviations of daily mean temperatures about the monthly mean, and these were interpolated from station data for the baseline period and from daily model outputs for the driving HadAM3H-A2 simulation for the future scenarios (standard deviations deviate little from those from the RCMs nested in this model).

The following crop-specific temperature requirements were adopted:

- Grain maize (*Zea mays*): 693°Cd above a base temperature of 10°C, accumulated throughout the year. This threshold was selected for individual years such that the zone in which the threshold is exceeded in nine out of ten years (90% reliability) matches the suitability zone based on period-mean climate above a higher threshold of 850°Cd, described in earlier work as corresponding to the requirement for the earliest-maturing maize varieties cultivated in France (Carter et al., 1991). Here we assumed, arbitrarily, that farmers would expect a 90% success rate for ripening of grain maize.

- Soya bean (*Glycine max*, variety Kingsoy): 1920°Cd above a base temperature of 6°C, accumulated during 15 April-30 September (Carter et al., 1991). Kingsoy is later maturing and has higher temperature requirements than many other varieties, so estimates do not cover the full geographical range of soya cultivation.

2.2.2 Thermal growing season

The thermal growing season is commonly defined as the period during which mean daily air temperatures remain above 5°C (Leemans and van den Born, 1994). It has been shown to provide a good approximation of the mean temperature at which significant growth and development proceeds across a range of plant species including trees, natural vegetation and agricultural crops (Carter, 1998). This measure is sufficient, on its own, to describe the growing season in cooler regions of Europe, where temperature, rather than moisture, is the dominant constraint on plant growth. As such, the focus of analysis for this index is on northern Europe[3]. We calculated the thermal growing season using 30-year mean monthly temperatures, which were converted to daily values using a sine-curve interpolation method (Brooks 1943). The growing season starts when daily mean temperature first exceeds the threshold for at least 5 consecutive days in the spring; however, to avoid selecting dates during short periods of spring warmth followed by renewed cold, it can only commence if no later month up to and including June has a mean monthly temperature below the threshold. The growing season ends the day when the 10-day running mean falls below the threshold again in the autumn. Note that this definition is applicable for period-mean temperatures, which normally describe a fairly smooth annual cycle..

2.2.3 Potential biomass

Potential biomass was estimated with the Miami Model (Lieth, 1975). The model is based on an empirical relationship between measurements of the net primary productivity (NPP) of natural vegetation (assumed to be in equilibrium with climate) and long term mean climate at 53 measurement sites distributed globally across four world regions. It is given as:

---

[3] Defined in this study as the region 4-32°E; 55-75°N (Ruosteenoja et al., this volume)

$$y = \min \left\{ \begin{array}{l} 3000/(1+\exp(1.315-0.119 \cdot tmp) \\ 3000 \cdot (1-\exp(-0.000664 \cdot pre) \end{array} \right\} \tag{1}$$

where y denotes net primary productivity (g DM $m^{-2} a^{-1}$), tmp mean annual temperature (°C) and

pre mean annual precipitation (mm). The Miami model generates a realistic pattern of global

NPP (Dai and Fung 1993), though it tends to overestimate productivity in the tropics (Schuur

2003).

2.2.4 Energy demand for cooling

As a rough indicator of the energy demand for household cooling on hot days we used cooling

degree-days (CDD), computed using the same method as ETS but for a base temperature of 18°C

cumulated throughout the year. This value has been adopted in several published studies (e.g.

NCDC, 2002; DoE, 1996).

3. Results

3.1 Crop suitability

3.1.1 Mean soya bean suitability

For the observed baseline temperature during 1961-1990, the areas fulfilling the condition of

thermal suitability for the cultivation of soya bean have their northern border in southern Europe

(Fig. 2, green areas). National statistics show the present-day cultivated area to be concentrated

in Mediterranean and southeast European countries, with some production in Austria, Slovenia,

Hungary and even the UK (Eurostat, 2005). Latitudinal and altitudinal shifts of the suitability

zone under climate scenarios for the period 2071-2100 are shown in the same figure. The

expansion common to nine RCM-based scenarios, all driven by the HadAM3H-A2 simulation

(Table 1), covers most of central Europe including large parts of France, Germany and Poland

(red area in Fig. 2a). The maximum expansion among these scenarios extends into England,

southern Sweden and Finland, thus describing an uncertainty range of up to c. 670 km (measured

at 25°E – blue area in Fig. 2a). The equivalent uncertainty range among six AOGCM-based

scenarios under A2 forcing is much wider, covering a distance of up to c. 1170 km (Fig. 2b). A

yet wider uncertainty range is obtained when AOGCM-based scenarios covering the four SRES

emission scenarios are applied (Fig. 2c), with a northward expansion of suitability ranging from

less than 100 km in some regions under the B1 scenario to shifts into central Sweden and Finland

under the A1FI scenario.

3.1.2 Reliability of grain maize suitability

Suitability limits for grain maize cultivation based on temperatures from individual years during

1961-1990, requiring successful attainment of the revised ETS threshold of 693°Cd in 90% of

years, are estimated to lie in the Netherlands, Germany and Poland (red area in Fig. 3a). These

lie a little to the north of the limits estimated for the 1951-1980 observed climate by Carter et al.

(1991), which in turn were reported to lie slightly to the north of the northern limit of

commercial cultivation inferred from national statistics and mapped distributions. Estimates of

future suitability for the period 2071-2100 using simulated changes in temperature relative to

1961-1990 from the REMO-H-A2 run (selected arbitrarily as a typical example), show a

northward shift of the 90% reliability limit by over 1000km at 25°E (green area in Figs. 3a and

3b). To compare the effect on future maize reliability of modelled changes in inter-annual

variability (IAV) of temperature, suitability has been estimated for modelled mean change in temperature, assuming no change in IAV from the control (Fig. 3a), and assuming modelled future IAV (Fig. 3b). There is a clear decrease in the area of 90% reliability when modelled IAV is applied, while the zone of lower reliability is enlarged (Fig. 3b). This implies an increase in IAV between the control and scenario run of REMO-H. The implication of this result is that the expansion of grain maize suitability is 4.5% smaller if the effect of modelled IAV is taken into account. The same feature of a future increase in IAV is observed in estimates based on projections from six other RCMs, the HadAM3H and the ARPEGE stretched-grid model, reducing the expansion by between 2.0 and 6.7%.

3.2 Thermal growing season

The length of the thermal growing season in northern Europe was computed for the observed baseline period 1961-1990 and for a range of RCM- and GCM-based scenarios (Table 1). The RegCM and PROMES model domains do not extend to the northernmost latitudes of Europe, so both RCMs were excluded from this analysis. Across the seven RCM-based scenarios driven by the HadAM3H-A2 AGCM, and averaged over the whole region, the growing season lengthens by between 39 and 47 days (Fig. 4a). Interestingly, the season lengthens by 48 days under the driving HadAM3H-A2 scenario, implying that all seven RCM simulations project reduced warming compared to the driving AGCM in the critical transition seasons of the year with temperatures close to 5°C (Fig. 4a). This reduced warming effect in the RCM outputs is found both at the start and at the end of the growing season (Fig. 4b). Other scenario groups show generally smaller increases in growing season length for B2 compared to A2 emissions scenarios, while ECHAM4-OPYC-driven RCM simulations display stronger increases than HadAM3H-driven runs. The six AOGCM and three ARPEGE stretched-grid simulations clearly

11

span a wider range of changes than the RCMs alone for A2 forcing, and the uncertainty range is widened further under AOGCM-based scenarios forced by all four SRES emission scenarios (22-86 days – Fig. 4a). There are stronger changes at the end of the growing season compared to the start under all scenarios.

3.3 Potential biomass

Modelled European net primary productivity (NPP) levels are shown in Fig. 5. For the 1961-1990 period the highest NPP was estimated for large parts of central Europe with values of more than 1200 g DM m^{-2} a^{-1} (Fig. 5a). The lowest estimates of less than 400 g DM m^{-2} a^{-1} in northernmost Europe are limited by temperature; southern European regions are limited by precipitation. Estimates were also made of baseline NPP using the direct outputs from the nine HadAM2-A2-driven RCMs for 1961-1990. This provides a simple, if demanding test of the performance of RCMs in simulating present-day climate. Comparisons of RCM-based NPP estimates to those based on observed climate indicate that very large discrepancies (of as much as ±80%) can be found in some regions for some scenarios (not shown). Sensitivity studies indicated that these discrepancies are largely due to biases in the model estimates of baseline precipitation. NPP was also estimated using a seven-model ensemble mean 1961-1990 climate for those RCMs giving coverage over the whole European region (not shown). When compared with the NPP estimated using 1961-1990 observed climate, regional discrepancies varied between -47.7% and 45.4%, although they were lower than 20% in most parts of the study region. This deviation is somewhat smaller compared to calculations from individual simulations, but the magnitude is still comparable to changes in NPP for the future scenario shown in Fig. 5b.

Estimates for 2071-2100 based on the same nine RCMs (using the delta change approach applied to baseline CRU observations), show increases in NPP in individual grid cells of up to 60% estimated for parts of northern Europe but decreases of up to -70% in southern Europe. Since there is substantial agreement in this regional pattern of response, it has been averaged across seven of the RCMs (excluding RegCM and PROMES which do not cover northern Europe) in Fig. 5b. The changes are of a similar magnitude to the NPP deviations noted between observed and modelled baseline climate. In the regions showing the largest increases (northern Europe[3]) and decreases (south-western Europe[4]) in NPP, regional averages show that the estimates based on the nine nested RCMs are scattered around those based on the driving HadAM3H-A2 model. This result contrasts to the systematically smaller changes found with RCM-based scenarios for some temperature-based indices (cf. Fig. 4), and can be explained by the dependence of this model on precipitation as well as temperature. B2-based scenarios generally show smaller changes than A2 for both RCMs and GCMs, with the widest range of changes spanned by the A1FI and B1 scenarios. NPP increases range from 18 to 48% for northern Europe, and some scenarios even show average increases over south-western Europe.

3.4 Energy demand for cooling

Potential energy demand for cooling systems is estimated with the simple index of cooling degree-days (CDD). Computations were carried out for temperatures from individual years, using the observed baseline mean and IAV, using modelled IAV superimposed on observed means for the 1961-1990 period (discussed below), and using modelled future IAV superimposed on baseline mean temperatures plus modelled delta change for 2071-2100. Estimates for the observed baseline (1961-1990) are highest in southern Spain, Portugal, Greece

---

[4] Defined in this study as the region 15°W-18°E; 35-45°N (Ruosteenoja et al., this volume)

and Turkey, where values can be more than 10 times higher than in most areas of central and northern Europe.

Estimates based on simulations from nine RCMs and their driving HadAM3H-A2 simulation are shown in Fig. 6 for the grid cells that contain the locations of five European cities. Estimates for baseline conditions are shown both for observed and direct modelled temperatures, and differences between these are a measure of RCM performance at simulating present-day temperatures. Departures can be quite large at locations where present-day values are already non-zero in all years (e.g. deviations from –44% to +25% were computed for Madrid). However, these are still dwarfed by the increases estimated under future climate (111-148% at Madrid).

Two locations, Helsinki and Sofia, show weaker increases for all nine RCM-based scenarios compared to the driving AGCM; the remaining three locations show weaker increases for eight of the nine. Values in the Strasbourg grid cell reach similar levels as those under the baseline conditions at Madrid, while both the London and Helsinki grid cells maintain a relatively modest potential cooling demand, slightly exceeding that in the Strasbourg grid cell under baseline conditions. The IAV differs considerably between the scenarios. At some locations, CDD estimates based on the temperature variability from the bounding AGCM and the RCMs display stronger IAV than those based on that observed. Future inter-annual variability of CDD increases at all locations, and is especially marked in the Strasbourg grid cell where the 10 to 90 percentile spans up to 750 degree-days.

4. Discussion

4.1 Key impacts

14

We have demonstrated the response of simple indices of resource potential to scenarios of future climate based on a range of different climate model projections, alternative scenario construction methods, and covering several impact sectors. The general pattern of impacts computed for these different scenarios confirmed results from purely climatological analyses (e.g. Christensen and Christensen, this volume), namely that estimates for RCM-based scenarios closely follow those obtained for the bounding AGCM. ECHAM4/OPYC3-driven RCM-based scenarios consistently gave stronger changes in the temperature-based impact indices than those driven by HadAM3H. Moreover, the range spanned for scenarios based on six AOGCMs for the SRES A2 emissions is wider than the RCM-based range for all impact indices, although there are some cases where the RCM range lies somewhat outside the low end of the AOGCM range (e.g., see Fig.4a).

Estimates for the period 2071-2100 show substantial changes in all analysed impact sectors with relatively large ranges of uncertainty attributable to the different climate scenarios. The northern limits of areas suitable for the cultivation of soya bean and grain maize were estimated to shift by several hundred kilometres, which is in agreement with earlier scenario analysis using the same impact models (Carter et al., 1991). An extension of the thermal growing season by three to twelve weeks is estimated, with slightly stronger changes in autumn than in spring, and increased energy demand for cooling is implied by the cooling degree-day calculations, with the largest absolute increases occurring in central and southern Europe. The only index incorporating both temperature and precipitation changes, the Miami Model, shows strong increases in NPP in northern Europe and the Alps, and decreases in the south. Note that the (positive) direct effects of increasing carbon dioxide concentration on photosynthesis and on water use efficiency are not accounted for in this version of the Miami Model.

4.2 Main conclusions

A primary objective of this study has been to investigate if RCM-based scenarios confer any additional value for impact assessment compared to GCM-based scenarios. We conclude that answers to this depend strongly on the impact models being applied and the specific goals being pursued. The impact models applied here make use of monthly or annual, though not daily data. Nevertheless, even at this temporal resolution it might be expected that certain sub-GCM-grid-scale processes would be captured by RCMs but not GCMs, especially in transition zones marked by sharp topographical or land/water surface characteristics, hence improving the reliability of projections. We have explored two possible measures of this reliability: RCM performance at reproducing observed climate, and discrepancies between projections from RCMs compared to the driving GCM. Overall, our results have drawn attention to four points of interest, concerning: (i) uncertainties expressed by RCMs; (ii) inter-annual variability, (iii) the use of direct RCM outputs, and (iv) possible systematic differences between RCM and GCM projections.

4.2.1 Uncertainties expressed by RCMs

The use of projections from nine RCMs driven by the same GCM provided a unique opportunity to intercompare estimates of impacts across the scenarios. Inter-scenario differences were found to be relatively small compared to the uncertainties introduced by adopting different GCMs and/or different emissions scenarios. Hence, the application of RCM-based scenarios alone is unlikely to embrace a representative range of possible future impacts. Regardless of their accuracy in downscaling GCM information, RCM projections are still heavily conditioned by the behaviour of the driving GCM.

4.2.2 Inter-annual variability

Our analysis demonstrates the importance of accounting for inter-annual variability in estimating future impacts. Temperature-based indices exhibited an increase in IAV in the future simulations compared to the baseline for all HadAM3H-A2-driven RCMs as well as the HadAM3H-A2 run itself. Here again, the RCM-based scenarios seem to reflect the bounding AGCM, though there are no comparably large sets of RCM runs for other driving models to verify this result. Some implications of increased IAV from our results include an enhanced increase in peak cooling demand in the hottest years, which might encourage the accelerated installation of cooling systems, and a reduction in the expansion of reliable crop cultivation under warming compared to that estimated for unchanged variability, which could enhance the risk of harvest losses for farmers operating near the northern or upland margins of suitability.

4.2.3 Direct use of RCM outputs

Another question posed in this study concerned the direct use of RCM outputs in impact assessment. A demanding test of a climate model is to compare impact model estimates based on simulated climate with those based on observed climate. If these correspond closely, there may be good grounds to apply direct model outputs for the future as well. However, where there are clear biases in the resulting impacts, a compromise is to apply the delta change approach to the observed baseline. Model biases have been reduced in RCM control runs compared to earlier studies (e.g. see Jacob et al., this volume), but our results for both cooling degree-days and (especially) the Miami Model suggest that biases are still too great to recommend using direct

RCM outputs in place of actual observations in impact studies, and that the delta change approach is still a preferred option.

4.2.4 Systematic differences between RCM and GCM projections

Several temperature-based indices showed stronger changes with the driving AGCM simulation, HadAM3H-A2, than with all or most of the RCM simulations that were nested in it. Possible explanations for the damping of temperature changes in RCM simulations could include the enhanced ability of the RCMs to account for surface water features such as lakes and inland seas that are poorly resolved by the AGCM, or improved representation of surface albedo effects, including snow and ice feedbacks. However, our analysis of one set of RCMs driven by a single AGCM is only suggestive. Comparable exercises are needed to examine multiple RCMs nested in a range of driving GCMs and in different regions of the world.

The one impact index presented in this paper that did not reveal such a relationship was the Miami Model of potential biomass, which uses both temperature and precipitation as input parameters. Unlike temperatures, precipitation changes from RCMs are distributed on either side of the changes simulated by the driving HadAM3H-A2, a result that is not unexpected considering the high internal variability of modelled precipitation. Nonetheless, if scenarios based on dynamical downscaling offer systematically different results than GCM-based scenarios, which are still by far the most commonly applied scenarios in impact studies, it follows that regardless of whether one believes that GCMs exaggerate or RCMs underestimate future temperature changes over Europe, it would be prudent to apply a mix of both GCM-based and RCM-based scenarios in future impact assessments.

Acknowledgements

References

Brooks CEP (1943) Interpolation tables for daily values of meteorological elements. *Quarterly Journal of the Royal Meteorological Society* 69: 160-162.

Carter TR (1998) Changes in the thermal growing season in Nordic countries during the past century and prospects for the future. *Agricultural and Food Science in Finland* 7: 161-179

Carter TR, Porter JH, Parry ML (1991) Climatic warming and crop potential in Europe: Prospects and uncertainties. *Global Environmental Change* 1: 291-312

Chmielewski F-M, Rotzer T (2001) Response of tree phenology to climate change across Europe. *Agricultural and Forest Meteorology* 108: 101–112

Christensen JH, Christensen OB (this volume)

Dai A, Fung IY (1993) Can climate variability contribute to the "missing" CO_2 sink? *Global Biogeochemical Cycles* 7(3): 599–609.

DoE (1996) *Review of the Potential Effects of Climate Change in the United Kingdom*, Second Report of the United Kingdom Climate Change Impacts Review Group, Department of the Environment, London, 250 pp.

Eurostat (2005) Online data portal of the Statistical Office of the European Communities, http://epp.eurostat.cec.eu.int [Path: Agriculture and fisheries > Data > Agriculture > Agricultural products > Crops products > Crops products (excluding fruits and vegetables) > Crop production > C1470 Soya bean]

Giorgi F, Hewitson B, Christensen JH, Hulme M, von Storch H, Whetton P, Jones R, Mearns L, Fu C (2001) Regional climate information – evaluation and projections. Chapter 10 in: Houghton J, *et al*. (eds.). *Climate Change 2001: The Scientific Basis*. Intergovernmental Panel on Climate Change, Cambridge University Press, pp. 583-638.

Hulme M, Barrow EM, Arnell N, Harrison PA, Downing TE, Johns TC (1999) Relative impacts of human-induced climate change and natural climate variability. *Nature* 397: 688-691.

IPCC (2001) *Climate Change 2001: Impacts, Adaptation, and Vulnerability. Contribution of Working Group II to the Third Assessment Report of the Intergovernmental Panel on Climate*

Change [McCarthy JJ, Canziani OF, Leary NA, Dokken DJ, White KS (eds)]. Cambridge University Press, Cambridge and New York, 1032 pp.

Jacob D, et al. (this volume)

Kauppi P, Posch M (1988) A case study of the effects of CO2-induced climatic warming on forest growth and the forest sector: A. Productivity reactions of northern boreal forests. In: Parry ML, Carter TR, Konijn NT (eds) *The Impact of Climatic Variations on Agriculture, Vol. 1: Assessments in Cool Temperate and Cold Regions*. Kluwer, Dordrecht, pp. 183-195.

Kundzewicz ZW, Parry ML, Cramer W, Holten J, Kaczmarek Z, Martens P, Nicholls RJ, Öquist M, Rounsevell MDA, Szolgay J (2001) Europe. Chapter 13 in: *Climate Change 2001: Vulnerability, Impacts and Adaptation* [McCarthy J, *et al*. (eds)]. Intergovernmental Panel on Climate Change, Cambridge University Press, pp. 641-692.

Leemans R, van den Born, GJ (1994) Determining the potential distribution of vegetation, crops and agricultural productivity. *Water, Air and Soil Pollution* 76: 133-161.

Lieth H (1975) Modeling the primary productivity of the world. In: Lieth H, Whittaker RH (eds) *Primary Productivity of the Biosphere*. Springer, New York, pp. 237-263

McAvaney BJ, Covey C, Joussaume S, Kattsov V, Kitoh A, Ogana W, Pitman AJ, Weaver AJ, Wood RA, Zhao Z-C (2001) Model evaluation. Chapter 8 in: Houghton J, et al. (eds.). *Climate Change 2001: The Scientific Basis*. Intergovernmental Panel on Climate Change, Cambridge University Press, pp. 471-523.

Mearns LO, Hulme M, Carter TR, Leemans R, Lal M, Whetton PH (2001) Climate scenario development. Chapter 13 in: Houghton J, et al. (eds.). *Climate Change 2001: The Scientific Basis*. Intergovernmental Panel on Climate Change, Cambridge University Press, pp. 739-768.

Menzel A, Jakobi G, Ahas R, Scheifinger H, Estrella N (2003) Variations of the climatological growing season (1951-2000) in Germany compared with other countries. *International Journal of Climatology* 23: 793-812.

NCDC (2002) State, regional, and national monthly cooling degree-days weighted by population (2000 census): 1971 – 2000 (and previous normals periods). *Historical Climatography Series* No. 5-2, National Climatic Data Center, National Oceanic and Atmospheric Administration, Asheville, NC, 16 pp.

New M, Hulme M, Jones PD (1999) Representing twentieth century space-time climate variability. Part 1: development of a 1961–90 mean monthly terrestrial climatology. *Journal of Climate* 12: 829–856

New M, Hulme M, Jones PD (2000) Representing twentieth century space-time climate variability. Part 2: development of 1901–96 monthly grids of terrestrial surface climate. *Journal of Climate* 13: 2217-2238

Olesen, J, et al. (this volume)

Parry M (ed.) (2000) *Assessment of Potential Effects and Adaptations for Climate Change in Europe: The Europe ACACIA Project*. Jackson Environment Institute, University of East Anglia, Norwich, UK, 320 pp.

Ruosteenoja K, et al. (this volume)

Schuur EAG (2003) Productivity and global climate revisited: the sensitivity of tropical forest growth to precipitation. *Ecology* 84(5): 1165–1170

Walther G-R, Post E, Convey P, Menzel A, Parmesan C, Beebee TJC, Fromentin J-M, Hoegh-Guldberg IO, Bairlein F (2002) Ecological responses to recent climate change. *Nature* 416: 389-395

List of Tables

Table 1: List of climate model experiments, impact models, and impact experiments (see footnotes) applied in this paper. For more detailed information and full references to climate models, see Jacob et al. (this volume).

Climate models				Impact models			
Model acronym	Country of origin	Driving GCM	SRES emissions scenarios	Crop suitability	Thermal growing season	Miami Model (NPP)	Cooling degree-days
Regional climate model (RCM)							
HIRHAM	Denmark	H	A2	2,3,4,5	2,3,4	1,2,3,4	1,2,3,4,5
HIRHAM	Denmark	E	A2, B2	2,3,4,5	2,3,4	1,2,3,4	1,2,3,4,5
HadRM3H	UK	H	A2	2,3,4,5	2,3,4	1,2,3,4	1,2,3,4,5
CHRM	Switzerland	H	A2	2,3,4,5	2,3,4	1,2,3,4	1,2,3,4,5
CLM	Germany	H	A2	2,3,4,5	2,3,4	1,2,3,4	1,2,3,4,5
PROMES	Spain	H	A2, B2	2,3,4	-	1,2,3,4	1,2,3,4,5
RegCM	Italy	H	A2, B2	2,3,4	-	1,2,3,4	1,2,3,4,5
REMO	Germany	H	A2	2,3,4,5	2,3,4	1,2,3,4	1,2,3,4,5
RCAO	Sweden	H	A2, B2	2,3,4,5	2,3,4	1,2,3,4	1,2,3,4,5
RCAO	Sweden	E	A2, B2	2,3,4,5	2,3,4	1,2,3,4	1,2,3,4,5
RACMO2	Netherlands	H	A2	2,3,4,5	2,3,4	1,2,3,4	1,2,3,4,5
Atmospheric general circulation model (AGCM)							
HadAM3H (= H)	UK	HC	A2	2,3,4,5	2,3,4	1,2,3,4	1,2,3,4,5
Arpège*	France	HC	A2, B2	2,3,4,5	3,4	1,3,4	-
Atmosphere-ocean general circulation model (AOGCM)							
HadCM3 (= HC)	UK	-	Four‡	2,3,4	3,4	1,3,4	-
ECHAM4/OPYC3 (= E)	Germany	-	Four‡	2,3,4	3,4	1,3,4	-
CSIRO-MK2	Australia	-	Four‡	2,3,4	3,4	1,3,4	-
NCAR-PCM	USA	-	Four‡	2,3,4	3,4	1,3,4	-
CGCM2	Canada	-	Four‡	2,3,4	3,4	1,3,4	-
GFDL-R30	USA	-	Four‡	2,3,4	3,4	1,3,4	-

* Stretched-grid model, three ensemble members; ‡ A2, B2 (modelled) and A1FI, B1 (pattern-scaled); 1 direct climate model output vs. delta change approach; 2 differences between the driving AGCM and the RCM runs; 3 model range vs. range of emission scenarios; 4 changes in long-term mean climate; 5 changes in inter-annual climate variability

List of Figures

Figure 1. Changes of June-August mean temperature and annual precipitation by 2071-2100 relative to 1961-1990 averaged over northern and southern Europe from RCMs nested in HadAM3H-A2, from six AOGCMs under A2 forcing, and from the pattern-scaled outputs of six AOGCMs for SRES emissions scenarios A1FI, B1 and B2. Nine RCMs are considered for southern Europe ($35.0 - 47.5°$N; $15.0°$W $- 35.0°$E) and seven for northern Europe ($47.5 - 75.0°$N; $15.0°$W $- 35.0°$E), as the domains of the RegCM and PROMES models do not extend to high latitudes. For other model details, see Table 1 and Jacob et al. (this volume).

Figure 2. Modelled suitability for soya bean (var. Kingsoy) cultivation during the baseline (1961-1990 based on observed temperatures) and future (2071-2100) periods for: (a) nine RCM scenarios driven by HadAM3H for the SRES A2 scenario, (b) six AOGCM-A2 scenarios and (c) 24 AOGCM scenarios (SRES A1FI, A2, B1 and B2). Green areas show the suitable area for the baseline, red depicts the expansion common under all scenarios and blue the uncertainty range spanned by the minimum and maximum expansion of the scenarios in the respective group. Grey areas are unsuitable under all scenarios.

Figure 3. Zones of estimated grain maize reliability based on the REMO-H-A2 projection for 2071-2100. The effect on future reliability of accounting for changes in inter-annual variability (IAV) is examined by adjusting the observed 30-year mean 1961-1990 temperatures according to delta changes from REMO, and superimposing modelled 1961-1990 IAV in (a) and modelled future IAV in (b). Red areas show 90% reliability under observed baseline temperatures.

Figure 4. Regionally-averaged changes in (a) the length, and (b) the start (bottom) and end (top) of the thermal growing season in northern Europe[3] for different groups of climate scenarios from

RCM, AGCM and AOGCM simulations for the period 2071-2100 compared with the baseline (1961-1990). All scenarios are applied as delta changes to the CRU baseline temperatures.

Figure 5. Net primary productivity (NPP) computed using the Miami Model: (a) observed baseline climate (1961-1990), (b) mean of estimates of percentage change in NPP between 1961-1990 and 2071-2100 for seven RCM-based scenarios driven by the HadAM3H-A2 simulation (excluding RegCM and PROMES).

Figure 6. Cooling degree-days in individual land grid cells representing five European cities. Lower symbols are estimates of means assuming 1961-1990 observed mean temperature and inter-annual variability (triangles) and observed mean temperature and modelled IAV (circles). Crosses show estimates based on modelled 1961-1990 temperatures. Upper symbols are based on model projections (squares) for 2071-2100. The method of computation is the same as described in the caption to Figure 3. Models are the driving HadAM3H-A2 simulation (open symbols) and nine RCMs nested within it (solid symbols). Error bars show 10 and 90 percentiles of the 30-year estimates.
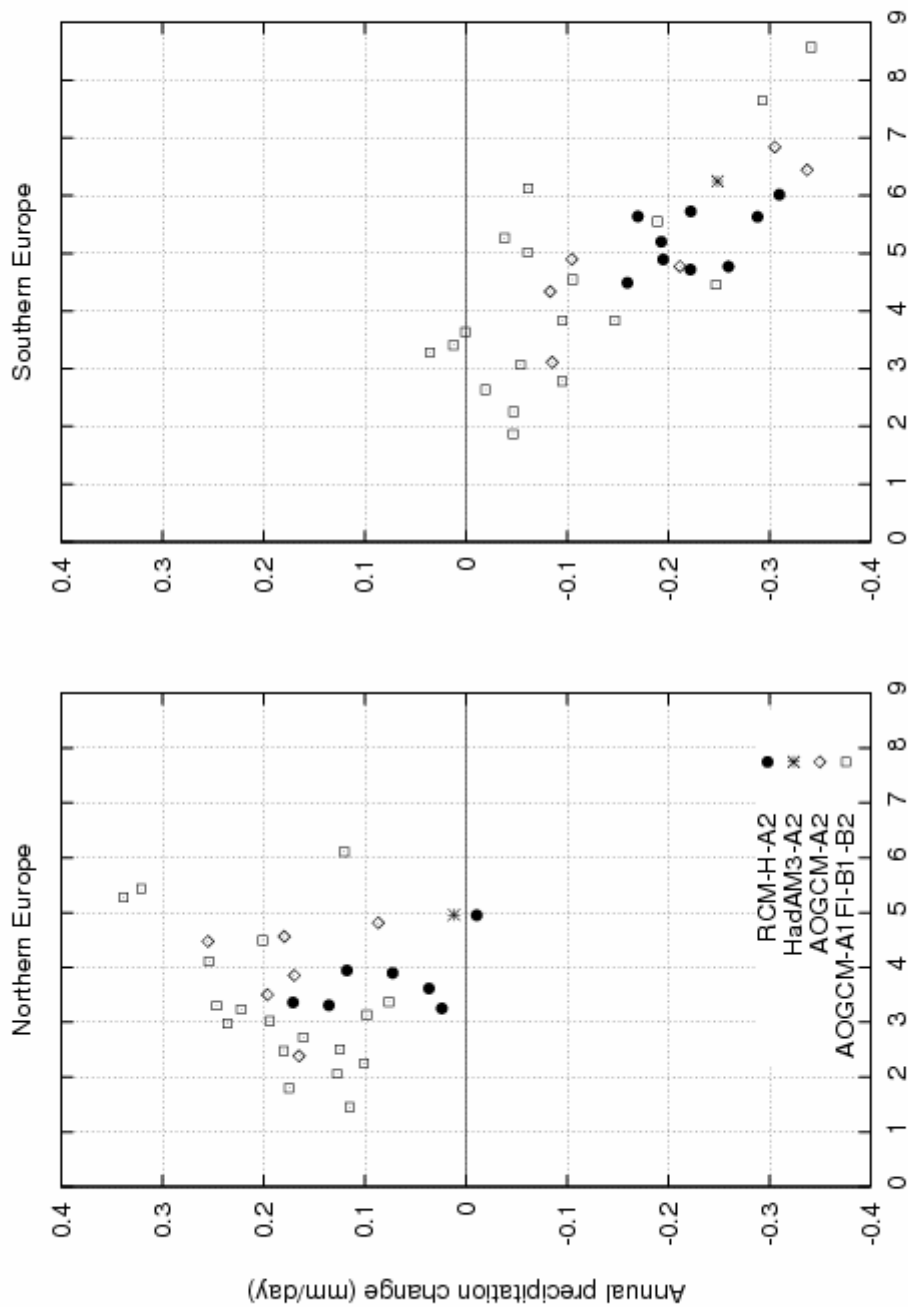
Figure 1. Changes of June-August mean temperature and annual precipitation by 2071-2100 relative to 1961-1990 averaged over northern and southern Europe from RCMs nested in HadAM3H-A2, from six AOGCMs under A2 forcing, and from the pattern-scaled outputs of six AOGCMs for SRES emissions scenarios A1FI, B1 and B2. Nine RCMs are considered for southern Europe (35.0 − 47.5°N; 15.0°W − 35.0°E) and seven for northern Europe (47.5 − 75.0°N; 15.0°W − 35.0°E), as the domains of the RegCM and PROMES models do not extend to high latitudes. For other model details, see Table 1 and Jacob et al. (this volume).

27

(a) 9 RCMs, HC-A2   (b) 6 GCMs, A2   (c) 6 GCMs
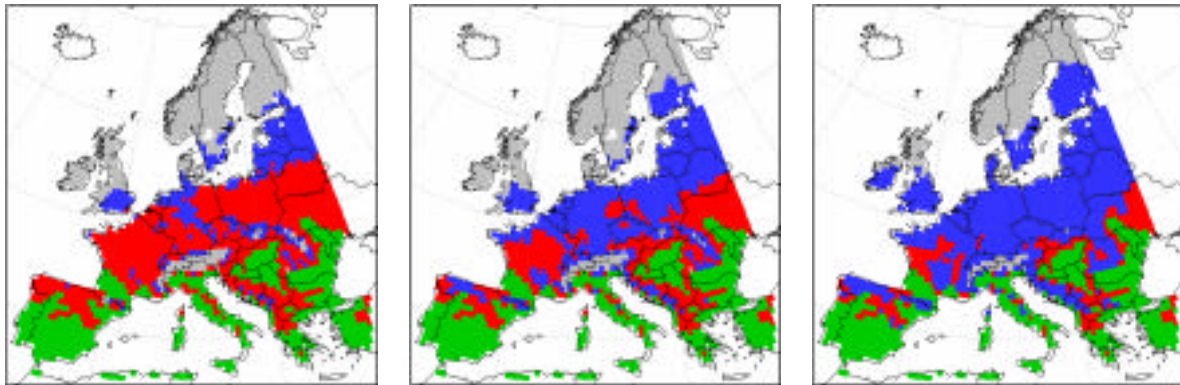
A1FI, A2, B1, B2

Figure 2. Modelled suitability for soya bean (var. Kingsoy) cultivation during the baseline (1961-1990 based on observed temperatures) and future (2071-2100) periods for: (a) nine RCM scenarios driven by HadAM3H for the SRES A2 scenario, (b) six AOGCM-A2 scenarios and (c) 24 AOGCM scenarios (SRES A1FI, A2, B1 and B2). Green areas show the suitable area for the baseline, red depicts the expansion common under all scenarios and blue the uncertainty range spanned by the minimum and maximum expansion of the scenarios in the respective group. Grey areas are unsuitable under all scenarios.

(a) Baseline + REMO ?T;

REMO 1961-1990 IAV

(b) Baseline + REMO ?T;

REMO 2071-2100 IAV

Modelled

- **> 90%** (green)
- **51-90%** (dark blue)
- **11-50%** (orange)
- **1-10%** (yellow)
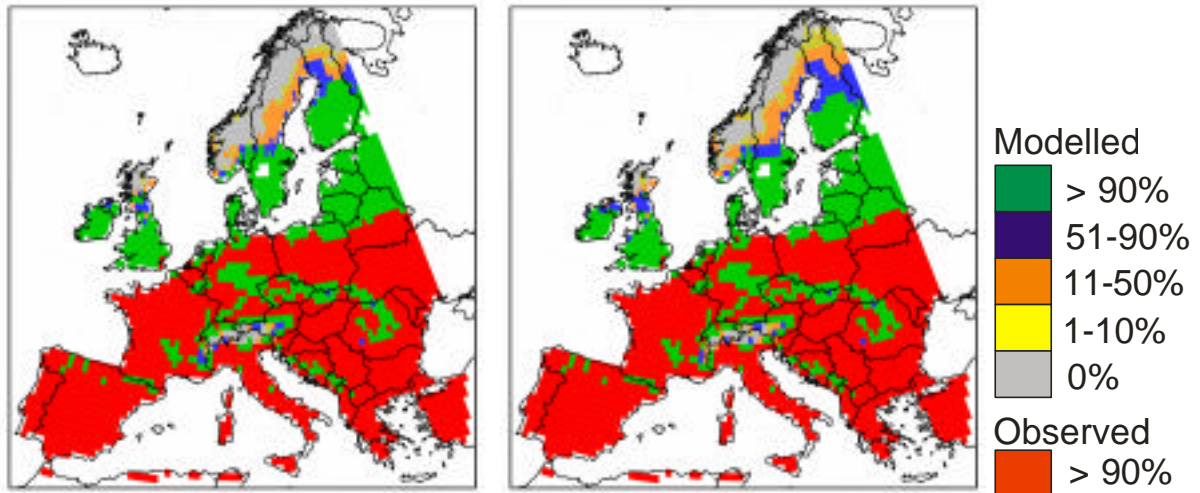- **0%** (grey)

Observed

- **> 90%** (red)

Figure 3. Zones of estimated grain maize reliability based on the REMO-H-A2 projection for 2071-2100. The effect on future reliability of accounting for changes in inter-annual variability (IAV) is examined by adjusting the observed 30-year mean 1961-1990 temperatures according to delta changes from REMO, and superimposing modelled 1961-1990 IAV in (a) and modelled future IAV in (b). Red areas show 90% reliability under observed baseline temperatures.
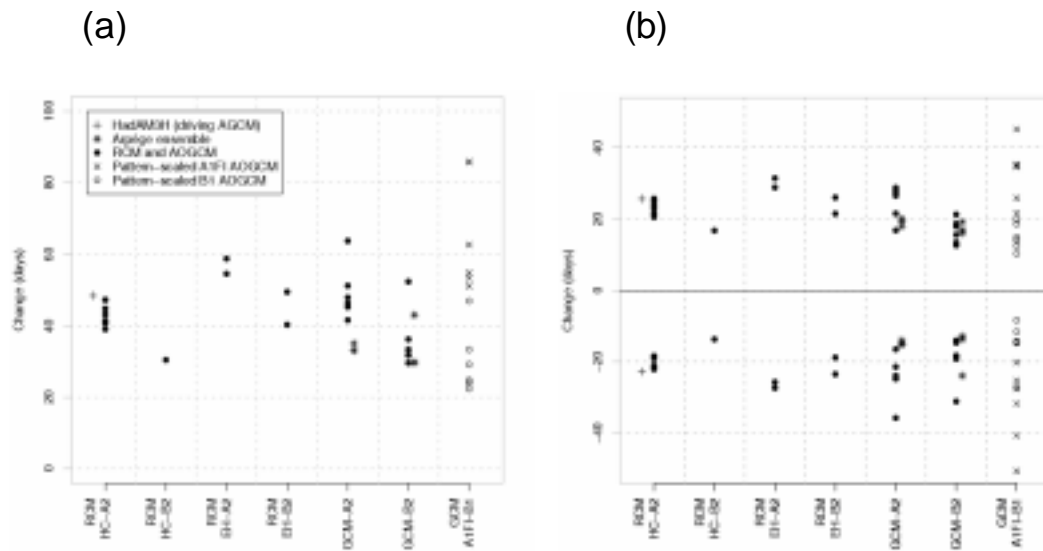
Figure 4. Regionally-averaged changes in (a) the length, and (b) the start (bottom) and end (top) of the thermal growing season in northern Europe[5] for different groups of climate scenarios from RCM, AGCM and AOGCM simulations for the period 2071-2100 compared with the baseline (1961-1990). All scenarios are applied as delta changes to the CRU baseline temperatures.

---

[5] Defined in this study as the region 4-32°E; 55-75°N (Ruosteenoja et al., this volume)

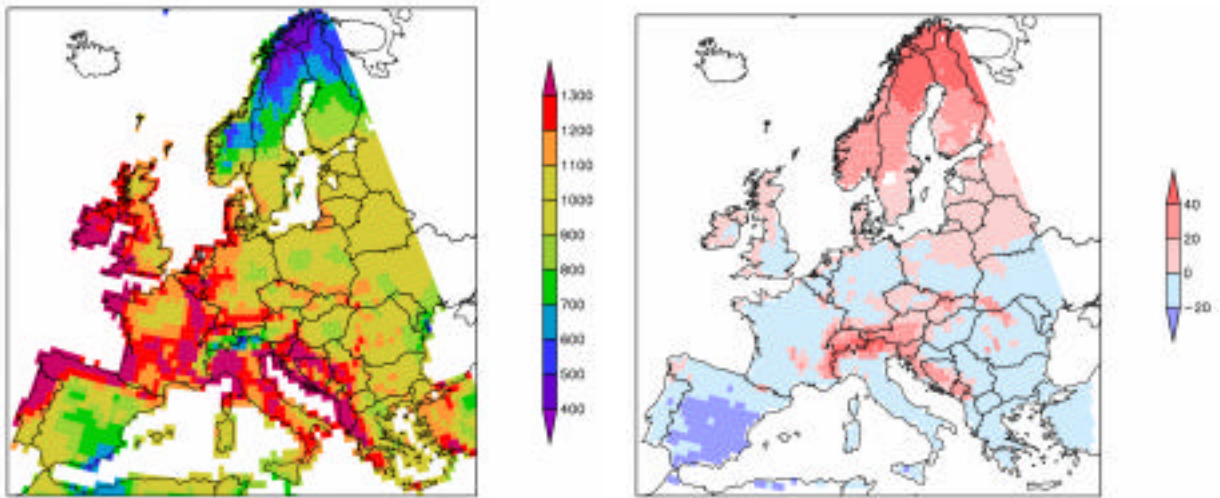(a) Baseline (g DM m^{-2} a^{-1})   (b) 7 RCMs: 2071-2100 (change, %)

Figure 5. Net primary productivity (NPP) computed using the Miami Model: (a) observed baseline climate (1961-1990), (b) mean of estimates of percentage change in NPP between 1961-1990 and 2071-2100 for seven RCM-based scenarios driven by the HadAM3H-A2 simulation (excluding RegCM and PROMES).
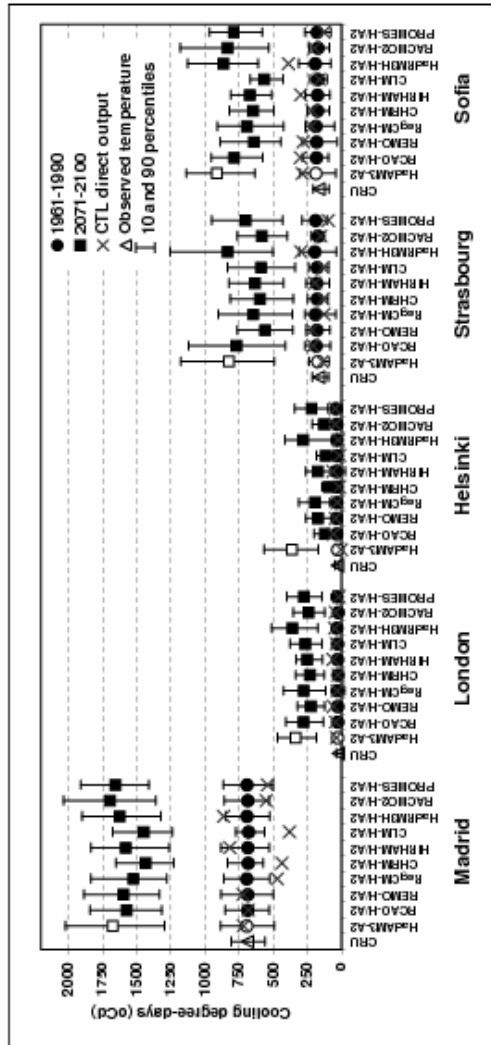
Figure 6. Cooling degree-days in individual land grid cells representing five European cities. Lower symbols are estimates of means assuming 1961-1990 observed mean temperature and inter-annual variability (triangles) and observed mean temperature and modelled IAV (circles). Crosses show estimates based on modelled 1961-1990 temperatures. Upper symbols are based on model projections (squares) for 2071-2100. The method of computation is the same as described in the caption to Figure 3. Models are the driving HadAM3H-A2 simulation (open symbols) and nine RCMs nested within it (solid symbols). Error bars show 10 and 90 percentiles of the 30-year estimates.